

Models and Benchmarks for Representation Learning of Partially Observed Subgraphs

Dongkwan Kim

dongkwan.kim@kaist.ac.kr

Korea Advanced Institute of Science and Technology
Daejeon, Republic of Korea

Jaimeen Ahn

jaimeen01@kaist.ac.kr

Korea Advanced Institute of Science and Technology
Daejeon, Republic of Korea

Jiho Jin

jinjh0123@kaist.ac.kr

Korea Advanced Institute of Science and Technology
Daejeon, Republic of Korea

Alice Oh

alice.oh@kaist.edu

Korea Advanced Institute of Science and Technology
Daejeon, Republic of Korea

ABSTRACT

Subgraphs are rich substructures in graphs, and their nodes and edges can be partially observed in real-world tasks. Under partial observation, existing node- or subgraph-level message-passing produces suboptimal representations. In this paper, we formulate a novel task of learning representations of partially observed subgraphs. To solve this problem, we propose Partial Subgraph InfoMax (PSI) framework and generalize existing InfoMax models, including DGI, InfoGraph, MVGRL, and GraphCL, into our framework. These models maximize the mutual information between the partial subgraph's summary and various substructures from nodes to full subgraphs. In addition, we suggest a novel two-stage model with k -hop PSI, which reconstructs the representation of the full subgraph and improves its expressiveness from different local-global structures. Under training and evaluation protocols designed for this problem, we conduct experiments on three real-world datasets and demonstrate that PSI models outperform baselines.

CCS CONCEPTS

• **Computing methodologies** → **Learning latent representations; Neural networks; Supervised learning by classification.**

KEYWORDS

graph neural networks; subgraph representation learning; mutual information maximization

ACM Reference Format:

Dongkwan Kim, Jiho Jin, Jaimeen Ahn, and Alice Oh. 2022. Models and Benchmarks for Representation Learning of Partially Observed Subgraphs. In *Proceedings of the 31st ACM International Conference on Information and Knowledge Management (CIKM '22)*, October 17–21, 2022, Atlanta, GA, USA. ACM, New York, NY, USA, 10 pages. <https://doi.org/10.1145/3511808.3557647>

Permission to make digital or hard copies of all or part of this work for personal or classroom use is granted without fee provided that copies are not made or distributed for profit or commercial advantage and that copies bear this notice and the full citation on the first page. Copyrights for components of this work owned by others than ACM must be honored. Abstracting with credit is permitted. To copy otherwise, or republish, to post on servers or to redistribute to lists, requires prior specific permission and/or a fee. Request permissions from [permissions@acm.org](https://permissions.acm.org).
CIKM '22, October 17–21, 2022, Atlanta, GA, USA.

© 2022 Association for Computing Machinery.
ACM ISBN 978-1-4503-9236-5/22/10...\$15.00
<https://doi.org/10.1145/3511808.3557647>

1 INTRODUCTION

The graph neural network (GNN) has become a major framework to learn representations of nodes, edges, and graphs [3, 8, 11, 19]. In addition, subgraphs can express various real-world data: news propagation in a social network or disease in a graph of symptoms [2].

The current formulation of subgraph representation learning by Alsentzer et al. [2] assumes full observation of nodes and edges in a subgraph, and that assumption often does not hold in the real world. If so, existing models may learn suboptimal representations because of inaccurate message-passing with missing nodes or edges. In this paper, we suggest a novel task of learning representations of partial subgraphs by relaxing the assumption of complete observation.

For this 'partial subgraph learning' task, we propose the *Partial Subgraph InfoMax* (PSI) framework based on mutual information (MI) maximization. Inspired by Deep InfoMax [18] that maximizes MI between the global summary (e.g., images) and local parts (e.g., patches), PSI maximizes MI between a partial subgraph and its substructures (e.g., nodes or full subgraphs). We generalize existing InfoMax models for node and graph-level tasks [16, 49, 55, 59] to solve the partial subgraph learning problem. PSI models first summarize a specific partial subgraph and learn to distinguish for its summary whether a substructure is related to the same subgraph (positive) or not (negative). This allows learning the structural hierarchy of nodes, partial and full subgraphs in subgraph representations.

However, the summary of the partial subgraph cannot explicitly encode missing information. Thus, we employ two-stage PSI models that reconstruct the summary close to the full subgraph under insufficient observation. We first propose ' k -hop PSI' that reconstructs the full subgraph by assembling k -hop neighbors of high MI with the partial subgraph. Then, the second PSI model takes the reconstructed subgraph summary as input and learns local-global structures different from the first k -hop PSI.

We demonstrate the improved representation learning performance of PSI models with experiments on three real-world datasets. These datasets simulate scenarios of fake news early detection, social network user profiling, and disease diagnosis with partial observation (Figure 1). Our models consistently outperform baseline models for all datasets. In addition, we analyze models' performance depending on the properties of subgraphs and the global graph.

We present the following contributions. First, we formulate the partial subgraph learning problem and suggest realistic training and evaluation protocols (§2). Second, we propose the Partial Subgraph

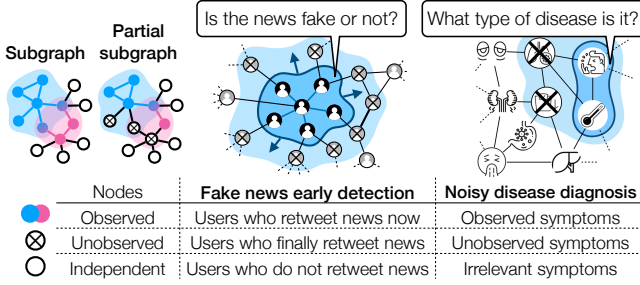


Figure 1: Left: Comparison of subgraph and partial subgraph representation learning. Middle & Right: Real-world examples (§2) of partial subgraph learning.

InfoMax framework for this problem (§3). Third, we demonstrate that our model outperforms baselines on three real-world datasets (§5). Our code is available at <https://github.com/dongkwan-kim/PSI>.

2 PARTIAL SUBGRAPH LEARNING PROBLEM

We formulate a novel problem of learning subgraph representations under partial observations of nodes and edges.

Notations. Let $\mathcal{G} = (\mathbb{V}^{\text{glob}}, \mathbb{A}^{\text{glob}})$ be a global graph, where \mathbb{V}^{glob} is a set of nodes and \mathbb{A}^{glob} is a set of edges, and $\mathbf{X}^{\text{glob}} \in \mathbb{R}^{|\mathbb{V}^{\text{glob}}| \times F}$ is a feature matrix of nodes. A subgraph $\mathcal{S} = (\mathbb{V}^{\text{sub}}, \mathbb{A}^{\text{sub}})$ of \mathcal{G} is defined as a graph, the nodes and edges of which are subsets of \mathbb{V}^{glob} and \mathbb{A}^{glob} respectively. Each subgraph has a label $y \in \{1, \dots, C\}$, and sometimes, a subgraph-level feature $\vec{g} \in \mathbb{R}^{F'}$ may exist.

Problem formulation. We formulate the ‘partial subgraph learning’ by relaxing the complete observation assumption of Alsentzer et al. [2], considering a subset of nodes or edges of the subgraph, as in Figure 1. We define a partial subgraph \mathcal{S}^{obs} of \mathcal{S} as $\mathcal{S}^{\text{obs}} = (\mathbb{V}^{\text{obs}}, \mathbb{A}^{\text{obs}})$ where $\mathbb{V}^{\text{obs}} \subset \mathbb{V}^{\text{sub}}$ and $\mathbb{A}^{\text{obs}} \subset \mathbb{A}^{\text{sub}}$. We denote a set of subgraphs as $\mathbb{S} = \{\mathcal{S}_1, \dots, \mathcal{S}_M\}$, and corresponding partial subgraphs as $\mathbb{S}^{\text{obs}} = \{\mathcal{S}_1^{\text{obs}}, \dots, \mathcal{S}_M^{\text{obs}}\}$, where each $\mathcal{S}_i^{\text{obs}}$ is a subgraph of \mathcal{S}_i for $i \in \{1, \dots, M\}$. We aim to learn a representation $\vec{s} \in \mathbb{R}^F$ for each $\mathcal{S}^{\text{obs}} \in \mathbb{S}^{\text{obs}}$ to predict y .

Real-world examples. One example of a real-world scenario is in detection of fake news in a social network, where the propagation tree of news can be represented as a subgraph. Rather than a fully propagated subgraph, it is more useful to detect fake news with an early propagated subgraph before the news spreads. Here, nodes are observed according to the order in which the information is propagated, and a partial subgraph would contain only nodes of the early propagation. Another example is a noisy diagnosis task of diseases (as subgraphs) based on a knowledge graph of symptoms (as nodes) [2]. In some cases, not all symptoms of the disease may appear or be seen, and a diagnosis is made based solely on the observed ones. The observation order of symptoms would not follow a fixed order but depend on the specific situation of the patient.

Realistic training and evaluation protocols. For training and evaluation, we create partial subgraphs by selecting nodes \mathbb{V}^{obs} from the nodes \mathbb{V}^{sub} of the full subgraph. We fix validation and test node sets with a *constant* size for each subgraph. This is more realistic than selecting nodes in proportion to the subgraph size (i.e., $|\mathbb{V}^{\text{sub}}|$) in that we cannot know the exact size at evaluation. We create a new partial subgraph of fixed size for training at every iteration. As we note above, there may be a specific observation ordering of the nodes. It is natural to take these into account when constructing

Table 1: The summary of differences between PSI models.

	PS-DGI	PS-MVGRL	PS-InfoGraph	PS-GraphCL
Substructures to maximize MI with partial subgraphs	Nodes in full subgraphs			Summary of full subgraphs
Negative samples	Row-wise shuffled nodes		Nodes in other subgraphs	
Graph augmentations	-	Personalized PageRank	-	Node dropping, edge perturbation, attribute masking
Shared encoders for partial & augmented subgraphs	N/A	False	N/A	True
MI estimator	GAN-like Divergence (GD)			InfoNCE

the partial subgraphs. Thus, we select early observed nodes if the observation is *ordered*, otherwise we sample the nodes randomly.

3 MODELS

We introduce the Partial Subgraph InfoMax (PSI) framework and its models. We first describe encoder-readout pipelines for learning subgraphs. Given a subgraph $(\mathbb{V}^*, \mathbb{A}^*)$ and features \mathbf{X}^{glob} , the GNN encoder \mathcal{E} outputs the node representations $\mathbf{H}^* = [\vec{h}_1 | \dots | \vec{h}_{|\mathbb{V}^*|}]^T \in \mathbb{R}^{|\mathbb{V}^*| \times F}$, and the readout \mathcal{R} generates the summary $\vec{s}^* \in \mathbb{R}^F$. Finally, the prediction function \mathcal{F} computes the logit $\vec{y} \in \mathbb{R}^C$. The superscript $*$ denotes the graph type as in §2 such as ‘sub’ for the full subgraph, ‘obs’ for the partial subgraph. This is summarized as:

$$(\mathbb{V}^*, \mathbb{A}^*, \mathbf{X}^{\text{glob}}) \xrightarrow{\mathcal{E}} \mathbf{H}^* \xrightarrow{\mathcal{R}} \vec{s}^* \xrightarrow{\mathcal{F}} \vec{y}. \quad (1)$$

3.1 Partial Subgraph InfoMax framework

The encoder-readout is insufficient for partial subgraph learning since only information from observed nodes is considered for prediction. Thus, we leverage a structural hierarchy from nodes to partial and full subgraphs using mutual information (MI) maximization. The PSI framework encodes the information of the full subgraph into the partial subgraph representation by maximizing MI between the partial subgraph summary \vec{s}^{obs} and representations from the full subgraph, nodes \mathbf{H}^{sub} or summary \vec{s}^{sub} .

Among several MI estimators modeled with neural networks [4], GAN-like divergence (GD) [40] and InfoNCE [42] estimators are widely used in InfoMax models for graphs. To maximize GAN-like divergence estimator between nodes \mathbf{H}^{sub} and the subgraph \vec{s}^{obs} , we minimize the following loss between samples from the joint distribution P and the product of marginal distributions $P \times \tilde{P}$:

$$\mathcal{L}^{\text{GD}} = -\mathbb{E}_P \left[\log \sigma \left(\mathcal{D}(\vec{h}_s, \vec{s}^{\text{obs}}) \right) \right] - \mathbb{E}_{P \times \tilde{P}} \left[\log \left(1 - \sigma \left(\mathcal{D}(\vec{h}_{\tilde{s}}, \vec{s}^{\text{obs}}) \right) \right) \right], \quad (2)$$

where s is an input sample from an empirical distribution P of the input space, \tilde{s} is a negative sample from \tilde{P} , \vec{s}^{obs} is the partial subgraph summary of s , \vec{h}_s is the node representation in s . A discriminator $\mathcal{D} : \mathbb{R}^F \times \mathbb{R}^F \rightarrow \mathbb{R}$ computes how much \vec{h}_s and \vec{s} are related. We also maximize the MI bound by minimizing InfoNCE loss,

$$\mathcal{L}^{\text{InfoNCE}} = \mathbb{E}_P \left[\mathcal{D}(\vec{h}_s, \vec{s}^{\text{obs}}) \right] - \mathbb{E}_{\tilde{P}} \left[\log \sum_{\tilde{s}} e^{\mathcal{D}(\vec{h}_{\tilde{s}}, \vec{s}^{\text{obs}})} \right]. \quad (3)$$

We generalize the following InfoMax models for learning partial subgraph representations: DGI [55], InfoGraph [49], MVGRL [16], and GraphCL [59] that maximize MI between local and global structures in the graph. Since they are designed for node or graph predictions, we incorporate them into PSI by considering each partial subgraph as an independent graph. Then, we jointly minimize the InfoMax loss and the cross-entropy loss $\mathcal{L}^{\text{graph}}$ on the logit \vec{y} and label y . See Table 1 for the architectures of PS-prefixed PSI models.

Table 2: Statistics of real-world datasets.

	FNTN	EM-User	HPO-Metab
# Global nodes	362,232	57,333	14,587
# Global edges	22,918,295	4,573,417	3,238,174
Density of \mathcal{G}	0.0002	0.0028	0.0304
# Subgraphs	1107	319	2397
# Nodes per subgraph	408.6 ± 386.7	155.4 ± 100.4	14.4 ± 6.2
# Edges per subgraph	412.9 ± 391.3	534.9 ± 645.3	181.3 ± 181.8
Density of \mathcal{S}	0.004 ± 0.003	0.016 ± 0.005	0.758 ± 0.149
# Classes	4	2	6

3.2 Two-Stage Models with k -hop PSI

Summarizing only nodes in the partial subgraph does not explicitly include all feature and structure information in the full subgraph. We propose k -hop PSI that reconstructs the full subgraph based on the partial subgraph’s k -hop neighborhoods using the MI estimator.

For subgraph reconstruction, k -hop PSI first inspects which nodes in \mathcal{G} belong to the full subgraph \mathcal{S} . However, \mathcal{G} is generally too big to fit in GPU memory, so we sample the k -hop neighbors $\mathcal{N}^k(\mathbb{V}^{\text{obs}})$ of the observed nodes. There are two kinds of nodes in k -hop neighbors: $\mathbb{V}^{\text{sub}k}$, nodes that are actually included in the full subgraph, and $\mathbb{V}^{\text{glob}k}$, nodes that are not. Formally,

$$\mathbb{V}^{\text{sub}k} = \mathcal{N}^k(\mathbb{V}^{\text{obs}}) \cap \mathbb{V}^{\text{sub}}, \quad \mathbb{V}^{\text{glob}k} = \mathcal{N}^k(\mathbb{V}^{\text{obs}}) \cap (\mathbb{V}^{\text{glob}} \setminus \mathbb{V}^{\text{sub}}).$$

Using the GD estimator, k -hop PSI maximizes MI between representations of \mathbb{V}^{sub} and \mathbb{S}^{obs} by using nodes in $\mathbb{V}^{\text{sub}k} (\subset \mathbb{V}^{\text{sub}})$ as positive samples and nodes in $\mathbb{V}^{\text{glob}k} (\subset \mathbb{V}^{\text{glob}})$ as negative samples.

The score $\mathcal{D}(\vec{h}_v, \vec{s}^{\text{obs}})$ in the GD estimator (Eq. 2) can be interpreted as the probability that the node belongs to the subgraph. Using scores $\vec{d}^{k\text{-hop}} = \mathcal{D}(\mathbf{H}^{k\text{-hop}}, \vec{s}^{\text{obs}})$ where $\mathbf{H}^{k\text{-hop}}$ are representations of $\mathcal{N}^k(\mathbb{V}^{\text{obs}})$, we create $\vec{s}^{k\text{-hop}}$ for the final prediction,

$$\vec{s}^{k\text{-hop}} = \text{softmax}(\vec{d}^{k\text{-hop}}_{[\text{idx}]}) \cdot \text{MLP}(\mathbf{H}^{k\text{-hop}}_{[\text{idx}]}, \text{idx} = \text{top}_k(\vec{d}^{k\text{-hop}})), \quad (4)$$

a weighted average of k -hop neighbors by top- k values of $\vec{d}^{k\text{-hop}}$, where idx are top- k node indices. This k -hop PSI’s pooling can be seen as a full subgraph reconstruction from the corrupted subgraph.

Although a summary from k -hop PSI is close to the full subgraph, its objective only relies on k -hop neighborhoods of the partial subgraph. For positive samples $\mathbb{V}^{\text{sub}k}$, we cannot use the entire set of nodes \mathbb{V}^{sub} in the full subgraph if $\mathbb{V}^{\text{sub}k} \neq \mathbb{V}^{\text{sub}}$. In addition, the similar set of negative samples within k -hop will be drawn for each training iteration. To overcome this limitation, we propose two-stage models that link k -hop PSI with other PSI models. First, k -hop PSI produces the InfoMax loss $\mathcal{L}^{k\text{-hop}}$ and the summary $\vec{s}^{k\text{-hop}}$. We adopt the second PSI model, which uses this summary as input to distinguish positive and negative samples. Then, we compute the second InfoMax loss $\mathcal{L}^{2\text{nd}}$. Finally, we jointly minimize all losses including $\mathcal{L}^{\text{graph}}$, that is, $\mathcal{L}^{\text{graph}} + \lambda^{k\text{-hop}} \mathcal{L}^{k\text{-hop}} + \lambda^{2\text{nd}} \mathcal{L}^{2\text{nd}}$.

4 EXPERIMENTS

Datasets. We experiment with three real-world datasets. FNTN (Fake News in Twitter Network; ordered) [23, 30, 33–35] is a Twitter network (\mathcal{G}) with news propagation trees (\mathbb{S}), contents (\vec{g}), and genuineness (y). The fake news early detection task is classifying the genuineness of news by initial nodes. EM-User (Users in EndoMondo; unordered) [2, 38] is a fitness network of workouts (\mathcal{G}), users as subgraphs (\mathbb{S}), and their gender (y), where the task is to profile a user’s gender with only a few logs. The global graph \mathcal{G} of HPO-Metab (Metabolic disease in Human Phenotype Ontology;

unordered) [2, 15, 26, 37] is a knowledge graph of symptoms. Each subgraph \mathcal{S} is a collection of symptoms associated with a metabolic disease, and the label (y) is the disease type. The task is to classify the disease type, assuming only some of the symptoms are observed. Detailed statistics are reported in Table 2. We randomly split the train/val/test set of FNTN with a ratio of 70/15/15 and use public splits [2] for EM-User (70/15/15) and HPO-Metab (80/10/10).

Training and evaluation settings. For both training and evaluation, we set the number of observed nodes $|\mathbb{V}^{\text{obs}}|$ to 4 for HPO-Metab, (the average number of nodes < 16), and 8 for FNTN and EM-User, (the average size of subgraphs $\gg 16$). Further, to see the performance change with $|\mathbb{V}^{\text{obs}}|$, we conduct experiments where $|\mathbb{V}^{\text{obs}}|$ is 8, 16, 32, and 64 for FNTN and EM-User. We also experiment with an oracle setting where all subgraphs are fully observed.

Model and training details. For the encoder \mathcal{E} , we use the two-layer GraphSAGE [14] with skip connections [17]. As an input of \mathcal{E} , node features $\mathbf{X}^{\text{glob}} \in \mathbb{R}^{|\mathbb{V}^{\text{glob}}| \times F^{\text{in}}}$ are trainable parameters with F^{in} of 32 (FNTN) and 64 (others). For HPO-Metab and EM-User, we use pre-trained embeddings from Alsentzer et al. [2]. We use readout \mathcal{R} of mean pooling after a two-layer MLP for all models except for k -hop PSI in the two-stage model, where we use the soft-attention pooling [29] after a two-layer Transformer [53]. We add the positional encoding before Transformer for ordered FNTN. For the discriminator \mathcal{D} , we use a bilinear scoring [42, 55] for the GD estimator, and cosine similarity with a temperature [59] for the InfoNCE estimator. For the prediction function \mathcal{F} , we use a single-layer neural network. If there is a subgraph-level feature $\vec{g} \in \mathbb{R}^{F'}$, we first transform it to the vector of the same length as \vec{s} , concatenate it with \vec{s} , and feed them to the prediction layer. All models use $F = 64$ features, the ReLU activation, dropout of 0.2 [48], and the Adam optimizer [24] with a learning rate of 10^{-3} . We sample nodes in a one-hop neighborhood in the k -hop PSI (i.e., $k = 1$). They are implemented with PyTorch ecosystems [12, 13, 44, 63].

Two-stage models. We use k -hop PSI + PS-DGI and + PS-InfoGraph only for two-stage models since using PS-MVGRL or PS-GraphCL as a second model is practically difficult. For MVGRL, using non-shared encoders and PPR augmentation requires significant memory and computations, and for GraphCL, a large batch size is needed.

Baselines. All baselines share the following encoder-readout architecture: $\mathbf{H} = \mathcal{E}^B(\mathbf{X}[\mathbb{V}^{\text{obs}}], \mathbb{A}^{\text{obs}})$, $\vec{s}^B = \mathcal{R}^B(\mathbf{H})$, $\vec{y} = \mathcal{F}(\vec{s}^B, [\vec{g}])$, where \mathcal{E}^B are two-layer MLP, GCN [25], GraphSAGE [14], GAT [54], and SubGNN [2] with skip connections. We set \mathcal{R}^B the two-layer MLP after mean pooling for SubGNN and mean pooling after two-layer MLP for others. We report the performance of SubGNN on EM-User and HPO-Metab only since SubGNN requires large memory of $O(|\mathbb{V}^{\text{glob}}|^2)$ ($> 1\text{TB}$ for FNTN) in computing shortest paths.

5 RESULTS AND DISCUSSIONS

Performance by models and datasets. Table 3 summarizes the mean accuracies over five runs of various models. We confirm that PSI models outperform all comparison models for all three datasets except for PS-DGI and k -hop PSI. PS-DGI performs worse than the best baseline in EM-User and HPO-Metab. Among PSI models, PS-InfoGraph and PS-GraphCL consistently outperform baselines across datasets. PS-MVGRL shows the best performance among single PSI models on FNTN, but it does not fit in single GPU (VRAM of 11G) on EM-User. However, the performance differences among

Table 3: Mean and standard deviation of accuracy of five runs. The first column is the number of observed nodes $|\mathbb{V}^{\text{obs}}|$ (§4), and the setting of each dataset is indicated with †, ‡. The PSI model that outperforms the best baseline (except for the oracle) is indicated by color, and statistical significance by unpaired *t*-test by asterisks ($p < .001$, $*p < .1$).**

$ \mathbb{V}^{\text{obs}} $	Model	FNTN [‡]	EM-User [‡]	HPO-Metab [†]
100%	GraphSAGE	86.3 \pm 0.7	82.1 \pm 1.2	47.7 \pm 3.3
	MLP	82.5 \pm 2.6	71.9 \pm 4.6	43.5 \pm 4.4
	GCN	84.6 \pm 2.0	72.8 \pm 3.8	42.9 \pm 1.8
	GraphSAGE	84.9 \pm 1.3	68.1 \pm 2.6	44.1 \pm 1.3
	GAT	85.1 \pm 0.8	71.5 \pm 5.7	43.1 \pm 2.3
	SubGNN	N/A	61.3 \pm 5.4	37.1 \pm 1.5
	PS-DGI	87.5 \pm 1.2	72.3 \pm 6.2	44.0 \pm 1.8
	PS-InfoGraph	87.3 \pm 0.0	75.7 \pm 3.9	47.1 \pm 2.1
8 [‡] , 4 [†]	PS-MVGRL	88.6 \pm 0.9	OOM	45.4 \pm 2.4
	PS-GraphCL	88.1 \pm 1.3	75.3 \pm 2.4	47.2 \pm 3.5
	<i>k</i> -hop PSI	87.8 \pm 1.2	75.3 \pm 2.4	42.4 \pm 2.6
	<i>k</i> -hop PSI + PS-DGI	88.0 \pm 0.7	75.7 \pm 4.4	43.6 \pm 1.0
	<i>k</i> -hop PSI + PS-InfoGraph	89.6 \pm 1.8	77.0 \pm 5.2	44.6 \pm 1.6

the PSI models except for *k*-hop PSI are not statistically significant (p -value $> .1$ for all datasets in one-way ANOVA).

In FNTN and EM-User, *k*-hop PSI is on par with other PSI models, but in HPO-Metab, *k*-hop PSI significantly underperforms. This behavior is caused by differences in the density of the global graph. As in Table 2, HPO-Metab has a higher density (0.03) than FNTN (2×10^{-4}) and EM-User (2.8×10^{-3}). When *k*-hop subgraph sampling is used, more neighbor nodes are included for denser graphs. Since most of the sampled neighbors are not in the subgraph, it is difficult to distinguish which of many neighbors belong to the subgraph by the discriminator \mathcal{D} in *k*-hop PSI. It degrades the performance of discriminator \mathcal{D} and the classification performance eventually.

Two-stage model’s performance is mainly driven by the *k*-hop PSI’s performance. In HPO-Metab where *k*-hop PSI does not perform well, the performance is lower than single PSIs; otherwise, it outperforms single models. The noise from high density is still relevant in two-stage models. In all datasets, a two-stage model results in better performance than a single *k*-hop PSI, and the combination with PS-InfoGraph performed better than with PS-DGI.

Finally, we discuss the results of baselines. First, SubGNN underperforms simple models. SubGNN uses message-passing between subgraphs, and thus partial observation degrades its performance. Second, there is no significance difference in MLP, GCN, GraphSAGE, and GAT (p -value $> .1$ in one-way ANOVA).

Performance by the number of observed nodes. In Figure 2a, we show the mean accuracy of *k*-hop PSI + PS-InfoGraph (5 runs) by the number of observed nodes in training and test. We exclude HPO-Metab with an average number of nodes fewer than 64. Intuitively, more observations should result in better prediction, and the performance on EM-User is consistent with that intuition. However, for FNTN, the opposite is true because initial nodes are relatively important for the propagation-based fake news detection [5]. Note that adding observed nodes is equivalent to adding *k*-hop neighbors to be discriminated by \mathcal{D} in *k*-hop PSI. That is, the impact of performance degradation from neighborhood noise is more significant than information gain from additional nodes in FNTN.

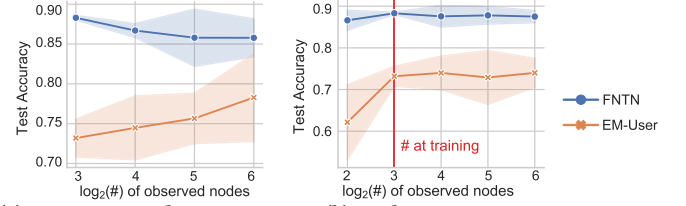


Figure 2: Performance of the *k*-hop PSI + PS-InfoGraph by the number of observed nodes at specific stages.

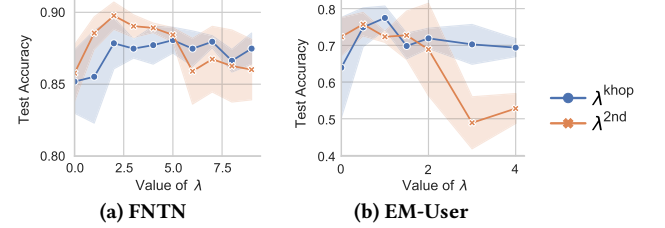


Figure 3: Mean and standard deviation of test accuracy (5 runs) on FNTN and EM-User against $\lambda^{k\text{-hop}}$ and $\lambda^{2\text{nd}}$.

Generalization across sizes of test subgraphs. Figure 2b shows how *k*-hop PSI + PS-InfoGraph generalizes across sizes of test subgraphs (mean performance over 5 runs). We set the number of *test* observed nodes from 4 to 64 and fix the number of *training* observed nodes to 8. Our model generalizes on test samples with more observed nodes (> 8) than training, but the variance of performances increases. In contrast, there is a lack of generalizability for test samples with fewer observed nodes than in the training stage. In particular, some trials do not converge on EM-User.

Sensitivity to λ . In Figure 3, we plot the test accuracy on FNTN and EM-User against $\lambda^{k\text{-hop}}$ (with *k*-hop PSI) and $\lambda^{2\text{nd}}$ (with *k*-hop PSI + PS-InfoGraph). The sensitivity to $\lambda^{2\text{nd}}$ is higher than $\lambda^{k\text{-hop}}$ in both datasets. Notably, in the region where $\lambda^{k\text{-hop}}$ is larger than the optimum, the performance fluctuates slightly less. A large $\lambda^{k\text{-hop}}$ makes the discriminator \mathcal{D} of *k*-hop PSI overestimate the probability of belonging to the subgraph. Since we only use a fixed ratio in the top_{*k*} pooling, those classified as nodes belonging to the subgraph more than this ratio are not involved in subgraph representations, thus no significant change where $\lambda^{k\text{-hop}}$ is large.

6 CONCLUSION

We explored the ‘partial subgraph learning task’ where only a part of the subgraph is observed. This is a more realistic and challenging scenario of subgraph representation learning. We also proposed a novel framework, Partial Subgraph Infomax (PSI), which maximizes the mutual information between the partial subgraph’s summary and representations of substructures like nodes or full subgraphs. Using training and evaluation protocols designed to simulate real-world use cases, PSI models outperform baselines in three datasets. One limitation is that *k*-hop PSI uses a naive *k*-hop sampling to select neighbors to be included in the subgraph, which is a major cause of performance degradation in dense graphs. We leave how to effectively and efficiently choose nodes as future work.

ACKNOWLEDGMENTS

This research was supported by the ERC Program through the NRF funded by the Korean Government MSIT (NRF-2018R1A5A1059921).

REFERENCES

- [1] Takuya Akiba, Shotaro Sano, Toshihiko Yanase, Takeru Ohta, and Masanori Koyama. 2019. Optuna: A next-generation hyperparameter optimization framework. In *KDD*. 2623–2631.
- [2] Emily Alsentzer, Samuel G Finlayson, Michelle M Li, and Marinka Zitnik. 2020. Subgraph Neural Networks. *NeurIPS* (2020).
- [3] Peter W Battaglia, Jessica B Hamrick, Victor Bapst, Alvaro Sanchez-Gonzalez, Vinicius Zambaldi, Mateusz Malinowski, Andrea Tacchetti, David Raposo, Adam Santoro, Ryan Faulkner, et al. 2018. Relational inductive biases, deep learning, and graph networks. *arXiv preprint arXiv:1806.01261* (2018).
- [4] Mohamed Ishmael Belghazi, Aristide Baratin, Sai Rajeshwar, Sherjil Ozair, Yoshua Bengio, Aaron Courville, and Devon Hjelm. 2018. Mutual information neural estimation. In *ICML*. PMLR, 531–540.
- [5] Tian Bian, Xi Xiao, Tingyang Xu, Peilin Zhao, Wenbing Huang, Yu Rong, and Junzhou Huang. 2020. Rumor detection on social media with bi-directional graph convolutional networks. In *AAAI*, Vol. 34. 549–556.
- [6] Antoine Bordes, Sumit Chopra, and Jason Weston. 2014. Question Answering with Subgraph Embeddings. In *Proceedings of the 2014 Conference on Empirical Methods in Natural Language Processing (EMNLP)*. 615–620.
- [7] Giorgos Bouritsas, Fabrizio Frasca, Stefanos Zafeiriou, and Michael M Bronstein. 2020. Improving graph neural network expressivity via subgraph isomorphism counting. *arXiv preprint arXiv:2006.09252* (2020).
- [8] Michael M Bronstein, Joan Bruna, Yann LeCun, Arthur Szlam, and Pierre Vandergheynst. 2017. Geometric deep learning: going beyond euclidean data. *IEEE Signal Processing Magazine* 34, 4 (2017), 18–42.
- [9] Jiangxia Cao, Xixun Lin, Shu Guo, Luchen Liu, Tingwen Liu, and Bin Wang. 2021. Bipartite Graph Embedding via Mutual Information Maximization. In *WSDM*. 635–643.
- [10] Wei-Lin Chiang, Xuanqing Liu, Si Si, Yang Li, Samy Bengio, and Cho-Jui Hsieh. 2019. Cluster-gcn: An efficient algorithm for training deep and large graph convolutional networks. In *KDD*. 257–266.
- [11] Vijay Prakash Dwivedi, Chaitanya K Joshi, Thomas Laurent, Yoshua Bengio, and Xavier Bresson. 2020. Benchmarking graph neural networks. *arXiv preprint arXiv:2003.00982* (2020).
- [12] William Falcon and The PyTorch Lightning team. 2019. *PyTorch Lightning*. <https://doi.org/10.5281/zenodo.3828935>
- [13] Matthias Fey and Jan E. Lenssen. 2019. Fast Graph Representation Learning with PyTorch Geometric. In *ICLR Workshop on Representation Learning on Graphs and Manifolds*.
- [14] William L Hamilton, Rex Ying, and Jure Leskovec. 2017. Inductive representation learning on large graphs. In *NeurIPS*. 1025–1035.
- [15] Taila Hartley, Gabrielle Lemire, Kristin D Kernohan, Heather E Howley, David R Adams, and Kym M Boycott. 2020. New diagnostic approaches for undiagnosed rare genetic diseases. *Annual review of genomics and human genetics* 21 (2020), 351–372.
- [16] Kaveh Hassani and Amir Hosein Khasahmadi. 2020. Contrastive multi-view representation learning on graphs. In *ICML*. PMLR, 4116–4126.
- [17] Kaiming He, Xiangyu Zhang, Shaoqing Ren, and Jian Sun. 2016. Deep residual learning for image recognition. In *Proceedings of the IEEE conference on computer vision and pattern recognition*. 770–778.
- [18] R Devon Hjelm, Alex Fedorov, Samuel Lavoie-Marchildon, Karan Grewal, Phil Bachman, Adam Trischler, and Yoshua Bengio. 2019. Learning deep representations by mutual information estimation and maximization. In *ICLR*.
- [19] Weihua Hu, Matthias Fey, Marinka Zitnik, Yuxiao Dong, Hongyu Ren, Bowen Liu, Michele Catasta, and Jure Leskovec. 2020. Open graph benchmark: Datasets for machine learning on graphs. *arXiv preprint arXiv:2005.00687* (2020).
- [20] Kexin Huang and Marinka Zitnik. 2020. Graph meta learning via local subgraphs. *NeurIPS* 33 (2020).
- [21] Yizhu Jiao, Yun Xiong, Jiawei Zhang, Yao Zhang, Tianqi Zhang, and Yangyong Zhu. 2020. Sub-graph Contrast for Scalable Self-Supervised Graph Representation Learning. *arXiv preprint arXiv:2009.10273* (2020).
- [22] Baoyu Jing, Chanyoung Park, and Hanghang Tong. 2021. HDML: High-order Deep Multiplex Infomax. *arXiv preprint arXiv:2102.07810* (2021).
- [23] Jooyeon Kim, Dongkwan Kim, and Alice Oh. 2019. Homogeneity-based transmissive process to model true and false news in social networks. In *WSDM*.
- [24] Diederik P Kingma and Jimmy Ba. 2014. Adam: A method for stochastic optimization. *arXiv preprint arXiv:1412.6980* (2014).
- [25] Thomas N. Kipf and Max Welling. 2017. Semi-Supervised Classification with Graph Convolutional Networks. In *ICLR*.
- [26] Sebastian Köhler, Leigh Carmody, Nicole Vasilevsky, Julius O B Jacobsen, Daniel Danis, Jean-Philippe Gourdine, Michael Gargano, Nomi L Harris, Nicolas Matentzoglou, Julie A McMurphy, et al. 2019. Expansion of the Human Phenotype Ontology (HPO) knowledge base and resources. *Nucleic acids research* 47, D1 (2019), D1018–D1027.
- [27] Phuc H Le-Khac, Graham Healy, and Alan F Smeaton. 2020. Contrastive representation learning: A framework and review. *IEEE Access* (2020).
- [28] Maosen Li, Siheng Chen, Ya Zhang, and Ivor Tsang. 2020. Graph Cross Networks with Vertex Infomax Pooling. In *NeurIPS*, H. Larochelle, M. Ranzato, R. Hadsell, M. F. Balcan, and H. Lin (Eds.), Vol. 33. Curran Associates, Inc., 14093–14105.
- [29] Yujia Li, Daniel Tarlow, Marc Brockschmidt, and Richard Zemel. 2015. Gated graph sequence neural networks. *arXiv preprint arXiv:1511.05493* (2015).
- [30] Xiaomo Liu, Armineh Nourbakhsh, Quanzhi Li, Rui Fang, and Sameena Shah. 2015. Real-time rumor debunking on twitter. In *CIKM*. 1867–1870.
- [31] Xiao Liu, Fanjin Zhang, Zhenyu Hou, Zhaoyu Wang, Li Mian, Jing Zhang, and Jie Tang. 2020. Self-supervised learning: Generative or contrastive. *arXiv preprint arXiv:2006.08218* 1, 2 (2020).
- [32] Dongsheng Luo, Wei Cheng, Dongkuan Xu, Wenchao Yu, Bo Zong, Haifeng Chen, and Xiang Zhang. 2020. Parameterized Explainer for Graph Neural Network. *NeurIPS* 33 (2020).
- [33] Jing Ma, Wei Gao, Prasenjit Mitra, Sejeong Kwon, Bernard J Jansen, Kam-Fai Wong, and Meeyoung Cha. 2016. Detecting rumors from microblogs with recurrent neural networks.(2016). In *IJCAI*. 3818–3824.
- [34] Jing Ma, Wei Gao, and Kam-Fai Wong. 2017. Detect Rumors in Microblog Posts Using Propagation Structure via Kernel Learning. In *ACL*. 708–717.
- [35] Jing Ma, Wei Gao, and Kam-Fai Wong. 2018. Rumor Detection on Twitter with Tree-structured Recursive Neural Networks. In *ACL*. 1980–1989.
- [36] Changping Meng, S Chandra Mouli, Bruno Ribeiro, and Jennifer Neville. 2018. Subgraph pattern neural networks for high-order graph evolution prediction. In *AAAI*, Vol. 32.
- [37] Dylan Mordaunt, David Cox, and Maria Fuller. 2020. Metabolomics to improve the diagnostic efficiency of inborn errors of metabolism. *International journal of molecular sciences* 21, 4 (2020), 1195.
- [38] Jianmo Ni, Larry Muhlestein, and Julian McAuley. 2019. Modeling Heart Rate and Activity Data for Personalized Fitness Recommendation. In *The Web Conference*. 1343–1353.
- [39] Mathias Niepert, Mohamed Ahmed, and Konstantin Kutzkov. 2016. Learning convolutional neural networks for graphs. In *ICML*. PMLR, 2014–2023.
- [40] Sebastian Nowozin, Botond Cseke, and Ryota Tomioka. 2016. f-GAN: Training Generative Neural Samplers using Variational Divergence Minimization. In *NeurIPS*, Vol. 29.
- [41] Hyun Oh Song, Yu Xiang, Stefanie Jegelka, and Silvio Savarese. 2016. Deep metric learning via lifted structured feature embedding. In *Proceedings of the IEEE conference on computer vision and pattern recognition*. 4004–4012.
- [42] Aaron van den Oord, Yazhe Li, and Oriol Vinyals. 2018. Representation learning with contrastive predictive coding. *arXiv preprint arXiv:1807.03748* (2018).
- [43] Chanyoung Park, Donghyun Kim, Jiawei Han, and Hwanjo Yu. 2020. Unsupervised attributed multiplex network embedding. In *AAAI*, Vol. 34. 5371–5378.
- [44] Adam Paszke, Sam Gross, Francisco Massa, Adam Lerer, James Bradbury, Gregory Chanan, Trevor Killeen, Zeming Lin, Natalia Gimelshein, Luca Antiga, et al. 2019. Pytorch: An imperative style, high-performance deep learning library. In *NeurIPS*. 8026–8037.
- [45] Zhen Peng, Wenbing Huang, Minnan Luo, Qinghua Zheng, Yu Rong, Tingyang Xu, and Junzhou Huang. 2020. Graph representation learning via graphical mutual information maximization. In *The Web Conference*. 259–270.
- [46] Jiezhong Qiu, Qibin Chen, Yuxiao Dong, Jing Zhang, Hongxia Yang, Ming Ding, Kuanan Wang, and Jie Tang. 2020. Gcc: Graph contrastive coding for graph neural network pre-training. In *KDD*. 1150–1160.
- [47] Yu Rong, Wenbing Huang, Tingyang Xu, and Junzhou Huang. 2020. DropEdge: Towards Deep Graph Convolutional Networks on Node Classification. In *ICLR*.
- [48] Nitish Srivastava, Geoffrey Hinton, Alex Krizhevsky, Ilya Sutskever, and Ruslan Salakhutdinov. 2014. Dropout: A Simple Way to Prevent Neural Networks from Overfitting. *Journal of Machine Learning Research* 15, 56 (2014), 1929–1958.
- [49] Fan-Yun Sun, Jordan Hoffman, Vikas Verma, and Jian Tang. 2020. InfoGraph: Unsupervised and Semi-supervised Graph-Level Representation Learning via Mutual Information Maximization. In *ICLR*.
- [50] Qingyun Sun, Jianxin Li, Hao Peng, Jia Wu, Yuanxing Ning, Phillip S. Yu, and Lifang He. 2021. SUGAR: Subgraph Neural Network with Reinforcement Pooling and Self-Supervised Mutual Information Mechanism. *arXiv:2101.08170 [cs.LG]*
- [51] Komal Teru, Etienne Denis, and Will Hamilton. 2020. Inductive relation prediction by subgraph reasoning. In *ICML*. PMLR, 9448–9457.
- [52] Michael Tschannen, Josip Djolonga, Paul K. Rubenstein, Sylvain Gelly, and Mario Lucic. 2020. On Mutual Information Maximization for Representation Learning. In *ICLR*.
- [53] Ashish Vaswani, Noam Shazeer, Niki Parmar, Jakob Uszkoreit, Llion Jones, Aidan N Gomez, Lukasz Kaiser, and Illia Polosukhin. 2017. Attention is All you Need. *NeurIPS* 30 (2017), 5998–6008.
- [54] Petar Veličković, Guillem Cucurull, Arantxa Casanova, Adriana Romero, Pietro Liò, and Yoshua Bengio. 2018. Graph Attention Networks. In *ICLR*.
- [55] Petar Veličković, William Fedus, William L. Hamilton, Pietro Liò, Yoshua Bengio, and R Devon Hjelm. 2019. Deep Graph Infomax. In *ICLR*.
- [56] Pengyang Wang, Yanjie Fu, Yuanchun Zhou, Kunpeng Liu, Xiaolin Li, and Kien Hua. 2020. Exploiting mutual information for substructure-aware graph representation learning. In *IJCAI*. 3415–3421.
- [57] Mike Wu, Milan Mosse, Chengxu Zhuang, Daniel Yamins, and Noah Goodman. 2021. Conditional Negative Sampling for Contrastive Learning of Visual Representations. In *ICLR*.

- [58] Rex Ying, Dylan Bourgeois, Jiaxuan You, Marinka Zitnik, and Jure Leskovec. 2019. Gnnexplainer: Generating explanations for graph neural networks. *NeurIPS* (2019).
- [59] Yuning You, Tianlong Chen, Yongduo Sui, Ting Chen, Zhangyang Wang, and Yang Shen. 2020. Graph contrastive learning with augmentations. *NeurIPS* (2020).
- [60] Junchi Yu, Tingyang Xu, Yu Rong, Yatao Bian, Junzhou Huang, and Ran He. 2021. Graph Information Bottleneck for Subgraph Recognition. In *ICLR*.
- [61] Hanqing Zeng, Hongkuan Zhou, Ajitesh Srivastava, Rajgopal Kannan, and Viktor Prasanna. 2020. GraphSAINT: Graph Sampling Based Inductive Learning Method. In *ICLR*.
- [62] Muhan Zhang and Yixin Chen. 2018. Link prediction based on graph neural networks. In *NeurIPS*. 5171–5181.
- [63] Yanqiao Zhu, Yichen Xu, Qiang Liu, and Shu Wu. 2021. An Empirical Study of Graph Contrastive Learning. *arXiv.org* (Sept. 2021). arXiv:2109.01116v1 [cs.LG]
- [64] Chengxu Zhuang, Alex Lin Zhai, and Daniel Yamins. 2019. Local aggregation for unsupervised learning of visual embeddings. In *Proceedings of the IEEE/CVF International Conference on Computer Vision*. 6002–6012.

The Appendix is not peer-reviewed and not a part of the proceedings of the 31st ACM International Conference on Information and Knowledge Management.

A RELATED WORK

Our study tackles a generalized subgraph representation learning with contrastive learning by mutual information maximization. This section introduces these two research areas.

A.1 Subgraphs in graph representation learning

There have been several approaches to use the information in subgraphs to improve representation learning of graph-structured data. They employ subgraphs to build more expressive models for node and graph representations [7, 39, 60], improve the scalability of graph neural network (GNN) training [10, 14, 61], augment data for graphs [46, 59], and explain prediction results of GNNs [32, 58]. Another common approach is to learn (or meta-learn) nodes or edges of interest by fetching a local (or enclosing) subgraph around them [6, 20, 51, 62].

While these methods target node- or graph-level tasks, a few studies focus on the subgraph-level task. Meng et al. [36] classifies the subgraph evolution pattern for subgraphs induced by three or four nodes as inputs, but it does not learn the representation of subgraphs. Subgraph Neural Network (SubGNN) [2] is designed for subgraph-level classification with subgraph representation learning using their internal/external topology, positions, and connectivity. SubGNN assumes that all subgraphs are fully observed, whereas our model does not make this assumption.

A.2 Contrastive learning by mutual information maximization

Contrastive learning is a widely-used method for self- and unsupervised learning [27, 31]. This has been applied in various types of data such as language, nodes, and images. Within contrastive learning, InfoMax methods [18] have been proposed recently, leveraging the known structure of data while maximizing mutual information (MI) of input and encoded output. Specifically, they maximize MI between pairs of local (e.g., patches) and global (e.g., images) based on neural MI estimators [4, 40, 42].

For graphs, various inherent substructures can be used in the design of contrastive learning. For example, node representations can be obtained by maximizing MI between node-graph pairs [16, 22, 43, 55, 56], node-subgraph pairs [21, 28, 45], edge-edge pairs [45], subgraph-graph pairs [9]. Likewise, graph representations can be obtained by maximizing MI between node-graph pairs [16, 49], node-subgraph pairs [28], subgraph-graph pairs [50], and graph-graph pairs [59]. Our model families learn representations of partial subgraphs by maximizing MI with other substructures like nodes or full subgraphs. To the best of our knowledge, there is no InfoMax method designed to learn subgraph representation itself, regardless of the conditions of incomplete observations.

B DATASET PRE-PROCESSING DETAILS

For FNTN, a follower network was crawled through the Twitter API between October and November 2018 for users in the propagation trees (including leaf users) [23, 30, 33–35]. For deactivated accounts,

we reflect the following information that can be obtained from the tree. We collect and distribute these data under Twitter’s policies and agreements¹.

Datasets in this paper are pre-processed to remove any personally identifiable information of users in real-world services (Twitter for FNTN and Endomondo for EM-User). Users are fully anonymized and treated as consecutive integers. In addition, we take TF-IDF vectors of 2000 words for news content without stop-words. The fake news texts, which can be offensive, cannot be restored.

For all datasets, single node graphs are excluded (five subgraphs for EM-User and three subgraphs for HPO-Metab). The rests are the same as the original papers (See Kim et al. [23] for FNTN, and Alsentzer et al. [2] for EM-User and HPO-Metab).

The raw datasets of HPO-Metab and EM-User can be downloaded from SubGNN’s GitHub repository². The codes using Twitter API to construct FNTN are public in the GitHub Repository³.

C DETAILS OF THE PARTIAL SUBGRAPH INFOMAX FRAMEWORK

In addition to the description in the Table 1, we give more details of the PSI framework and models in it. We generalize existing InfoMax models for learning partial subgraph representations. We consider models that can maximize MI between local and global structures in the graph, including DGI [55], InfoGraph [49], MVGRL [16], and GraphCL [59]. Since they are initially designed for the node or graph-level prediction, we incorporate them into the PSI framework by revising the core steps of the encoder-readout pipeline. Specifically, we view each partial subgraph as an independent graph and generate its summary vector as described in steps 1 – 3 of Algorithm 1. We maximize the MI between the partial subgraph summary and other substructures in full subgraphs (step 4). We follow the original models for the rest of the architecture.

A visual summary of PSI models (PS-DGI, PS-InfoGraph, PS-MVGRL, PS-GraphCL, and k -hop PSI) is illustrated in Figure 4. We focus on (1) what substructure pairs are used to maximize MI, (2) how negative samples are drawn from \tilde{P} , and (3) what graph augmentation methods are used.

D DISCUSSION ON NEGATIVE SAMPLING IN k -HOP PSI

Using the GAN-like divergence estimator (Equation 2), k -hop PSI maximizes the MI between representations of \mathbb{V}^{sub} and \mathbb{S}^{obs} by using nodes in $\mathbb{V}^{\text{obs}} \cup \mathbb{V}^{\text{sub}k}$ as positive samples and nodes in $\mathbb{V}^{\text{glob}k}$ as negative samples, that is,

$$\mathcal{L}^{k\text{-hop}} = \frac{1}{|\mathbb{V}^{\text{obs}} \cup \mathbb{V}^{\text{sub}k} \cup \mathbb{V}^{\text{glob}k}|} \left[\sum_{\sigma \in \mathbb{V}^{\text{obs}} \cup \mathbb{V}^{\text{sub}k}} \log \sigma \left(\mathcal{D}(\vec{h}_\sigma, \vec{s}^{\text{obs}}) \right) + \sum_{\tilde{\sigma} \in \mathbb{V}^{\text{glob}k}} \log \left(1 - \sigma \left(\mathcal{D}(\vec{h}_{\tilde{\sigma}}, \vec{s}^{\text{obs}}) \right) \right) \right]. \quad (5)$$

In k -hop PSI, the negative nodes $\mathbb{V}^{\text{glob}k}$ are not sampled from the true marginal distribution. Intuitively, this $\mathbb{V}^{\text{glob}k}$, a set of nodes closely linked to the subgraph within k -hop, can be considered hard negative samples conditioned on positive samples. This approach is known to learn a better representation in contrastive and

¹<https://developer.twitter.com/en/developer-terms>

²<https://github.com/mims-harvard/SubGNN>

³<https://github.com/dongkwan-kim/Fake-News-Twitter-Network>

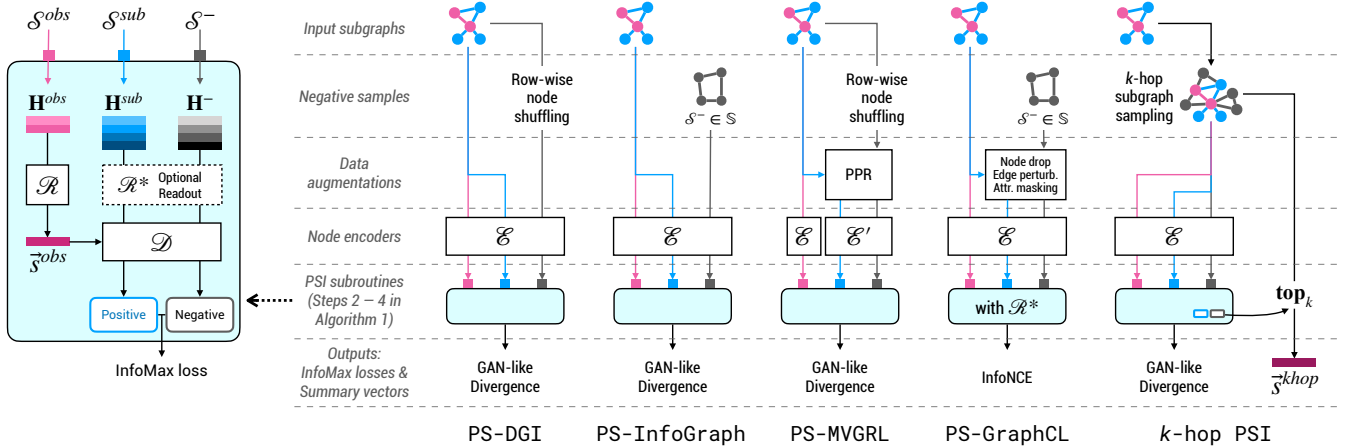


Figure 4: Models in the PSI framework: PS-DGI, PS-InfoGraph, PS-MVGRL, PS-GraphCL, and k -hop PSI.

Algorithm 1: Partial Subgraph InfoMax framework

Data: The global graph $\mathcal{G} = (\mathbb{V}^{\text{glob}}, \mathbb{A}^{\text{glob}})$, \mathbb{X}^{glob} and a partially observed subgraph \mathbb{S}^{obs} in \mathbb{S}^{obs} :
 $\mathbb{S}^{\text{obs}} = (\mathbb{V}^{\text{obs}}, \mathbb{A}^{\text{obs}})$, \vec{g} , $\mathbb{X}^{\text{obs}} = \mathbb{X}^{\text{glob}}[\mathbb{V}^{\text{obs}}]$

Result: A logit vector of \mathbb{S}^{obs} : $\vec{y} \in \mathbb{R}^C$.

1. Encode nodes in the partial subgraph:

$$\mathbb{H}^{\text{obs}} = \mathcal{E}(\mathbb{X}^{\text{obs}}, \mathbb{A}^{\text{obs}}).$$

2. Create the partial subgraph summary: $\vec{s}^{\text{obs}} = \mathcal{R}(\mathbb{H}^{\text{obs}})$.

3. Compute a logit vector: $\vec{y} = \mathcal{F}(\vec{s}^{\text{obs}}, [\vec{g}])$. We also use a subgraph-level feature \vec{g} in the final prediction if exists.

4. In the training stage, optimize losses to update parameters:

if training then

a. Draw negative subgraph(s): $\mathbb{S}^- = (\mathbb{V}^-, \mathbb{A}^-) \in \mathbb{S}$.

b. Augment full and negative subgraphs if necessary:

if graph augmentations are used then

$$\mathbb{S}^{\text{sub}}, \mathbb{S}^- = \text{Aug}(\mathbb{S}^{\text{sub}}), \text{Aug}(\mathbb{S}^-).$$

end

c. Encode nodes in full and negative subgraphs, then summarize them if necessary:

$$\mathbb{H}^{\text{sub}} = \mathcal{E}(\mathbb{X}[\mathbb{V}^{\text{sub}}], \mathbb{A}^{\text{sub}} \text{ or } \mathbb{A}^{\text{glob}}[\mathbb{V}^{\text{sub}}]),$$

$$\mathbb{H}^- = \mathcal{E}(\mathbb{X}[\mathbb{V}^-], \mathbb{A}^- \text{ or } \mathbb{A}^{\text{glob}}[\mathbb{V}^-]),$$

$$\vec{s}^{\text{sub}}, \vec{s}^- = \mathcal{R}(\mathbb{H}^{\text{sub}}), \mathcal{R}(\mathbb{H}^-).$$

d. Compute \mathcal{L}^{GD} or InfoNCE with the partial subgraph summary (\vec{s}^{obs}), positive (\mathbb{H}^{sub} or \vec{s}^{sub}) and negative (\mathbb{H}^- or \vec{s}^-) samples (Equations 2 or 3).

e. Compute the cross-entropy loss $\mathcal{L}^{\text{graph}}$ on the logit \vec{y} and label y , and minimize $\mathcal{L}^{\text{graph}} + \lambda \mathcal{L}^{\text{GD}}$ or InfoNCE .

end

metric learning [41, 42, 64], but such non-i.i.d sampling may break the assumption on the MI bound [52]. In Proposition 1, similar to Conditional-NCE (CNCE) [57], we prove that a specific choice of negative sample distribution forms the lower bound of the GAN-like divergence MI estimator.

PROPOSITION 1 (THE CONDITIONAL GAN-LIKE DIVERGENCE MI BOUND). For d -dimensional random variables X and Y with a joint distribution $p(x, y)$ and marginal distributions $p(x)$ and $p(y)$, fix any function $f : (X, Y) \rightarrow \mathbb{R}$ and realization x of X . Let $c_x =$

$\mathbb{E}_{y \sim p(y)} [e^{f(x, y)}]$, $\mathbb{B}_{c_x} \subset \mathbb{R}$ be strictly lower bounded by c_x , and $\mathbb{Y}_{c_x} = \{y | e^{f(x, y)} \in \mathbb{B}_{c_x}\}$ with an assumption of $p(\mathbb{Y}_{c_x}) > 0$. For \mathbb{Y}_r in the Borel σ -algebra over \mathbb{R}^d , let $q(Y \in \mathbb{Y}_r | X = x) = p(\mathbb{Y}_r | \mathbb{Y}_{c_x})$, then $\mathcal{I}^{\text{CGD}} \leq \mathcal{I}^{\text{GD}}$ where

$$\mathcal{I}^{\text{CGD}} = \mathbb{E}_{x, y \sim p(x, y)} [\log \sigma(f(x, y))] + \mathbb{E}_{x \sim p(x)} \mathbb{E}_{y \sim q(y|x)} [\log (1 - \sigma(f(x, y)))], \quad (6)$$

$$\mathcal{I}^{\text{GD}} = \mathbb{E}_{x, y \sim p(x, y)} [\log \sigma(f(x, y))] + \mathbb{E}_{x \sim p(x)} \mathbb{E}_{y \sim p(y)} [\log (1 - \sigma(f(x, y)))]. \quad (7)$$

PROOF. It suffices to show that $\mathbb{E}_{y \sim p(y)} [\log (1 + e^{f(x, y)})] \leq \mathbb{E}_{y \sim q(y|x)} [\log (1 + e^{f(x, y)})]$ for all x to prove $\mathcal{I}^{\text{CGD}} \leq \mathcal{I}^{\text{GD}}$, since,

$$\mathbb{E}_{y \sim p(y)} [\log (1 + e^{f(x, y)})] \leq \mathbb{E}_{y \sim q(y|x)} [\log (1 + e^{f(x, y)})] \quad (8)$$

$$\Rightarrow \mathbb{E}_{x \sim p(x), y \sim p(y)} [\log (1 + e^{f(x, y)})] \leq \mathbb{E}_{x \sim p(x), y \sim q(y|x)} [\log (1 + e^{f(x, y)})] \quad (9)$$

$$\Rightarrow \mathbb{E}_{x \sim p(x), y \sim q(y|x)} [\log (1 - \sigma(f(x, y)))] \leq \mathbb{E}_{x \sim p(x), y \sim p(y)} [\log (1 - \sigma(f(x, y)))] \quad (10)$$

$$\Rightarrow \mathcal{I}^{\text{CGD}} \leq \mathcal{I}^{\text{GD}} \quad (11)$$

We apply the similar technique in CNCE [57] to prove Equation 8. Using Jensen's inequality to the right-hand side and the fact that $\mathbb{E}_p(e^{f(x, y)}) \leq e^{f(x, y_c)}$ for $y_c \in \mathbb{Y}_{c_x}$,

$$\mathbb{E}_p [\log (1 + e^{f(x, y)})] \leq \log \mathbb{E}_p [1 + e^{f(x, y)}] \leq \log (1 + e^{f(x, y_c)}). \quad (12)$$

If we take the expectation $\mathbb{E}_{y \sim q(y|x)}$ on both sides, we get Equation 8. \square

After applying f to the training set, the CNCE uses a subset, the exponentiated similarity $e^{f(\cdot, \cdot)}$ of which is bigger than that of a certain percentile. Instead, we employ k -hop sampling, which uses hop distance as a proxy of embedding distance (or dissimilarity). This method assumes that the hop and embedding distances of nodes created by message-passing are highly correlated. It is more efficient than using the actual similarity since it does not evaluate f for all instances.

Table 4: Summary of accuracy (5 runs) of GraphSAGE model on three datasets with regard to the ratio of observed nodes at the training and test (i.e., $x\%$ setting).

The ratio of observed nodes	FNTN	EM-User	HPO-Metab
12.5%	85.9 ± 1.3	54.5 ± 19.4	34.2 ± 2.1
25%	86.3 ± 0.7	82.6 ± 3.5	41.2 ± 1.3
100%	86.3 ± 0.7	82.1 ± 1.2	47.7 ± 3.3

Table 5: Mean wall-clock time (seconds) per batch of the training process on real-world datasets.

Model	FNTN	EM-User	HPO-Metab
MLP	0.021	0.040	0.018
GraphSAGE	0.028	0.037	0.019
SubGNN	N/A	0.126	0.086
k -hop PSI	0.816	0.103	0.406
PS-InfoGraph	0.047	0.053	0.033
k -hop PSI + PS-InfoGraph	0.834	0.141	0.413

E MODEL, TRAINING, AND HYPERPARAMETER CONFIGURATIONS

E.1 Model and training details

In addition to the description in the main paper, we use the following model architectures and training methods:

- All the models are implemented with PyTorch [44], PyTorch Geometric [13], PyGCL [63] and PyTorch Lightning [12].
- When using a bidirectional encoder, half of the hidden feature of 64 is divided and used for each direction. That is, we use 32 for forward edges and 32 for reverse edges.
- For positional encoding, we follow the Transformer’s original formula [53] and set the maximum length of 20. Note that the number of observed nodes is 8. When the numbers of observed nodes are 16, 32, and 64, the maximum lengths are 36, 68, and 132, respectively.
- A fixed number (N^{obs}) of observed nodes is sampled at each iteration of the training stage. To add more randomness, we sample a random element from $\{N^{\text{obs}} - 2, N^{\text{obs}} - 1, N^{\text{obs}}, N^{\text{obs}} + 1, N^{\text{obs}} + 2\}$ first and select the observed nodes of that number.
- For the k -hop subgraph, we dropout these edges with the probability of p_d [47].
- The batch sizes are 16 for FNTN and 64 for others, using the gradient accumulation (16 for FNTN, 1 for EM-User, and 16 for HPO-Metab).
- All model parameters are trained with 16-bit precision supported by PyTorch Lightning [12].
- Each experiment is done on a single GPU. These GPUs are the GeForce GTX 1080Ti, GeForce RTX 2080Ti, and Quadro RTX 8000, but each experiment does not require a specific GPU type. One machine has a total of 40 – 48 cores of CPUs and 4 – 8 GPUs.

E.2 Hyperparameter selection

We tune a subset of hyperparameters with validation sets using Optuna [1]. We choose different tuning algorithms and subsets of hyperparameters depending on models and experiment conditions. For baselines (non-InfoMax models), only weight decay is

tuned. For SubGNN, we compare the model with all (neighborhood, structure, and position) channels and models with only one channel each. For each case, we tune weight decay, an aggregator for initializing component embedding, k for k -hop neighborhood of subgraph component, and numbers of structure anchor patches, border/internal position anchor patches, border/internal neighborhood anchor patches, and LSTM layers for structure anchor patch embedding. Lastly, we tune weight decay, λ s in MI losses, the ratio in top_k pooling, and DropEdge probability p_d of k -hop subgraph for our models.

We use the Tree-structured Parzen Estimator algorithm under a total budget of 50 runs for most experiments. For SubGNN, we choose the random search following the original implementation. Exceptionally, we perform a grid search to evaluate the performance by the number of observed nodes (Figures 2a and 2b). We run a total of 36 experiments on the space of three λ ($\{1.0, 2.0, 3.0\}$), three $\lambda^{k\text{-hop}}$ ($\{1.0, 2.0, 3.0\}$), two weight decay ($\{10^{-4}, 10^{-3}\}$ for FNTN and $\{10^{-6}, 10^{-5}\}$ for EM-User), and two pool ratio ($\{10^{-3}, 10^{-2}\}$). All hyperparameters are reported in the code.

F DISCUSSION ON PERFORMANCE BY THE NUMBER OF OBSERVED NODES

In Figure 2a, we show the performance of k -hop PSI + PS-InfoGraph depending on the number of observed nodes. By observing more nodes, the performance on EM-User increases but that on FNTN decreases. We claim that the impact of performance degradation from neighborhood noise is more significant than information gain from additional nodes in FNTN.

Where the boundary of the full subgraph is unknown, the increase in the number of observed nodes presents two challenges—first, the number of nodes in the sampled k -hop neighborhood increases. Second, the number of nodes in the subgraph but unknown yet to the model decreases. We expect that the performance increases when the information gained from the additional nodes exceeds the noises from the above challenges.

Next, we show that initial nodes are relatively important for FNTN dataset. In Table 4, we report the experimental result of the GraphSAGE model by the ratio of observed nodes. We call this the $x\%$ setting similar to the 100% setting but uses only $x\%$ of nodes in training and evaluation. We set x to 12.5, 25, and 100. As the number of observed nodes decreases, the performance of the GraphSAGE model for all datasets generally decreases. However, the degree varies by dataset. Compared to EM-User and HPO-Metab, additional observed nodes in FNTN do not significantly affect representation quality. This is in line with Bian et al. [5].

We demonstrate that the information gained from additional nodes in FNTN is relatively small. Considering the challenges from these additions, this explains why the performance on FNTN decreases as the number of observed nodes increases in Figure 2a.

G TRAINING TIME

In Table 5, we report the mean wall-clock time per batch of k -hop PSI, PS-InfoGraph, and their two-stage models using a single machine (40-core CPU with one GTX1080Ti GPU). For all experiments, we use a batch size of four.

The PS-InfoGraph does not differ much from the baseline MLP and GraphSAGE in training time. The overhead is below 0.03s for all datasets. However, the model using k -hop PSI shows a relatively large training time compared to others ($\times 3 - \times 30$). We confirm that most of the increments occur from k -hop sampling. The more edges (e.g., FNTN) or density (e.g., HPO-Metab) of the global graph, the more time it takes to run. The EM-User dataset with a relatively low value for these properties takes a similar training time to that of SubGNN.

H ETHICAL CONSIDERATIONS

Learning subgraphs requires collecting more attributes (i.e., a global graph plus subgraphs) than learning nodes, edges, and graphs. This could lead to privacy invasion depending on the use case. For example, if we set the global graph as a user network of a social media

like FNTN and EM-User, our model should follow up the entire network throughout its life cycle of training and evaluation.

Furthermore, a deeper understanding of the partial subgraph learning problem may enable harmful applications, such as tracking users on social media. Indeed, our study deals with the profiling task of users' gender (EM-User). Similar concerns are raised in the SubGNN paper, which proposed the original dataset (See Broader Impact section in Alsentzer et al. [2]). Also, while our model suggests the positive application of fake news detection, it leaves room for attacks to deceive. This is a general problem with any machine learning model, and thus researchers accessing and using this research must be mindful of potential harm.

Lastly, EM-User dataset simulates the prediction task of binary genders (male and female), but genders could be non-binary in reality. Future research should consider that EM-User is an oversimplified dataset for benchmarking purposes.